

## Brief report

## Biallelic TLR4 deficiency in humans

Melania Capitani, PhD,<sup>a</sup> Ahmad A. Al-Shaibi, MSc,<sup>b</sup> Sumeet Pandey, PhD,<sup>a</sup> Lisa Gartner, MSc,<sup>a</sup> Henry Taylor, MD,<sup>a,c</sup> Satanay Z. Hubrack, MS,<sup>b</sup> Nourhen Agrebi, PhD,<sup>b</sup> Muneera Jassim Al-Mohannadi, MD,<sup>d</sup> Saad Al Kaabi, MD,<sup>d</sup> Thomas Vogl, PhD,<sup>e</sup> Johannes Roth, MD,<sup>e</sup> Daniel Kotlarz, MD, PhD,<sup>f,g</sup> Christoph Klein, MD, PhD,<sup>f,h</sup> Adrian K. Charles, MD, FRCPath,<sup>i</sup> Vinayan Vijayakumar, MSc,<sup>j</sup> Mohammed Yousuf Karim, MBBChir, FRCPath,<sup>j</sup> Bruce George, MD,<sup>k</sup> Simon P. Travis, MD, PhD,<sup>a,l</sup> Mamoun Elawad, MD,<sup>m</sup> Bernice Lo, PhD,<sup>b,n\*</sup> and Holm H. Uhlig, MD, DPhil<sup>a,l,o\*</sup> Oxford and London, United Kingdom; Doha, Qatar; and Münster, Munich, and Neuherberg, Germany

**Background:** Toll-like receptors (TLRs) mediate functions for host defense and inflammatory responses. TLR4 recognizes LPS, a component of gram-negative bacteria as well as host-derived endogenous ligands such as S100A8 and S100A9 proteins.

**Objective:** We sought to report phenotype and cellular function of individuals with complete TLR4 deficiency.

**Methods:** We performed genome sequencing and investigated exome and genome sequencing databases. Cellular responses were studied on primary monocytes, macrophages, and neutrophils, as well as cell lines using flow cytometry, reporter, and cytokine assays.

**Results:** We identified 2 individuals in a family of Qatari origin carrying a homozygous stop codon variant p.Q188X in TLR4 presenting with a variable phenotype (asymptomatic and inflammatory bowel disease consistent with severe perianal Crohn disease). A third individual with homozygous p.Y794X was identified in a population database. In contrast to hypomorphic polymorphisms p.D299G and p.T399I, the variants p.Q188X and p.Y794X completely abrogated LPS-induced cytokine responses whereas TLR2 response was normal. TLR4 deficiency causes a neutrophil CD62L shedding

defect, whereas antimicrobial activity toward intracellular *Salmonella* was intact.

**Conclusions:** Biallelic TLR4 deficiency in humans causes an inborn error of immunity in responding to LPS. This complements the spectrum of known primary immunodeficiencies, in particular myeloid differentiation primary response 88 (MYD88) or the IL-1 receptor-associated kinase 4 (IRAK4) deficiency that are downstream of TLR4 and TLR2 signaling. (J Allergy Clin Immunol 2022;■■■■:■■■-■■■.)

**Key words:** Inflammatory bowel disease, primary immunodeficiency

## INTRODUCTION

Identification of microbes via pattern recognition receptors is a key requisite for protective inflammatory immune responses. Toll-like receptors (TLRs) are a group of intracellular and extracellular transmembrane pattern recognition receptors. TLR4 (CD284), expressed by immune and nonimmune cells, was the first identified member of the mammalian TLR family.<sup>1</sup>

From <sup>a</sup>the Translational Gastroenterology Unit, University of Oxford, Oxford, United Kingdom; <sup>b</sup>the Research Branch, Sidra Medicine, Doha; <sup>c</sup>the Department of Surgery and Cancer, Imperial College London, London; <sup>d</sup>Hamad Medical Center, Gastroenterology, Doha; <sup>e</sup>the Institute of Immunology, and Interdisciplinary Center for Clinical Research, University of Münster, Münster; <sup>f</sup>Dr. von Hauner Children's Hospital, Department of Pediatrics, University Hospital, LMU Munich, Munich; <sup>g</sup>Institute of Translational Genomics, Helmholtz Zentrum München, German Research Center for Environmental Health, Neuherberg; <sup>h</sup>Deutsche Zentrum für Infektionsforschung (DZIF) and Deutsches Zentrum für Kinder- und Jugendgesundheit, partner site Munich; <sup>i</sup>Anatomical Pathology, Sidra Medicine, and <sup>j</sup>Hematopathology, Sidra Medicine, Doha; <sup>k</sup>the Department of Colorectal Surgery and <sup>l</sup>the Oxford Biomedical Research Centre, University of Oxford, Oxford; <sup>m</sup>the Department of Gastroenterology, Sidra Medicine, Doha; <sup>n</sup>the College of Health and Life Sciences, Hamad Bin Khalifa University, Doha; and <sup>o</sup>the Department of Paediatrics, University of Oxford, Oxford.

\*These authors contributed equally to this work.

M.C., D.K., C.K., and H.H.U. are supported by The Leona M. and Harry B. Helmsley Charitable Trust (grant no. HBR02270). B.L. is supported by the Sidra Medicine Internal Research Fund (IRF-2017, SDR200018). H.H.U., S.P., and S.P.T. are supported by the Biomedical Research Centre (BRC), which is supported by the National Institute for Health Research (NIHR). The views expressed are those of the author(s) and not necessarily those of the National Health Service (NHS), the NIHR, or the Department of Health.

Disclosure of potential conflict of interest: H. H. Uhlig received research support or consultancy fees from Janssen, UCB Pharma, Eli Lilly, Pfizer, BMS/Celgene, Mestag, OMass, and AbbVie. S. P. Travis received research support from AbbVie, Buhlmann,

Celgene, IOIBD, Janssen, Lilly, Pfizer, Takeda, UCB, Vifor, and the Norman Collisson Foundation; consulting fees from AbbVie, Allergan, Abiomics, Amgen, Arena, Asahi, Astellas, Biocare, Biogen, Boehringer Ingelheim, Bristol-Myers Squibb, Buhlmann, Celgene, Chemocentryx, Cosmo, Enterome, Ferring, Giuliani SpA, GlaxoSmithKline (GSK), Genentech, Immunocore, Immunometabolism, Indigo, Janssen, Lexicon, Lilly, Merck, MSD, Neovacs, Novartis, NovoNordisk, NPS Pharmaceuticals, Pfizer, Proximagen, Receptos, Roche, Sensyne, Shire, Sigmoid Pharma, SynDermix, Takeda, Theravance, Tillotts, Topivert, UCB, VHSquared, Vifor, and Zeria; and speaker fees from AbbVie, Amgen, Biogen, Ferring, Janssen, Pfizer, Shire, Takeda, and UCB (no stocks or share options). M. Capitani is a current employee of SenTcell Ltd and S. Pandey of GSK. The rest of the authors declare that they have no relevant conflicts of interest.

Received for publication June 16, 2022; revised August 25, 2022; accepted for publication August 30, 2022.

Corresponding author: Bernice Lo, PhD, Translational Medicine Department, Sidra Medicine, Al Gharrafa Street, Ar-Rayyan, Doha, Qatar. E-mail: [blo@sidra.org](mailto:blo@sidra.org). Or: Holm H. Uhlig, MD, PhD, Translational Gastroenterology Unit and Department of Paediatrics, University of Oxford, John Radcliffe Hospital, Headley Way, Headington, Oxford OX3 9DU, UK. E-mail: [holm.uhlig@ndm.ox.ac.uk](mailto:holm.uhlig@ndm.ox.ac.uk). 0091-6749

© 2022 The Authors. Published by Elsevier Inc. on behalf of the American Academy of Allergy, Asthma & Immunology. This is an open access article under the CC BY license (<http://creativecommons.org/licenses/by/4.0/>).

<https://doi.org/10.1016/j.jaci.2022.08.030>

**Abbreviations used**

GnomAD: Genome Aggregation Database  
 IBD: Inflammatory bowel disease  
 LOF: Loss-of-function  
 MAF: Mean allele frequency  
 MD2: Myeloid differentiation factor 2  
 MYD88: Myeloid differentiation primary response 88  
 NF- $\kappa$ B: Nuclear factor kappa B  
 TLR: Toll-like receptor  
 WT: Wild-type

TLR4 is expressed not only by neutrophils, monocytes, and macrophages but also by nonhematopoietic cells such as fibroblasts and epithelial cells. TLR4 contains an extracellular leucine-rich repeat region, a helix transmembrane domain, and an intracellular Toll-IL-1 receptor domain. TLR4 binds the exogenous ligand LPS, derived from gram-negative bacteria, as well as endogenous ligands such as the antimicrobial protein complex S100A8/S100A9.<sup>2</sup>

The binding of LPS to TLR4 is mediated by its 2 coreceptors CD14 and MD-2. This binding initiates 2 intracellular signaling cascades: a myeloid differentiation primary response 88 (MYD88) and Toll-IL-1 receptor domain containing adaptor protein-dependent pathway that leads to nuclear factor kappa B (NF- $\kappa$ B) and activator protein 1 activation, with production of proinflammatory cytokines; and a second pathway, in which Toll-like receptor adaptor molecule/translocation-associated membrane protein recruitment activates interferon regulatory factor 3 and regulates transcription of type I interferons. CD14 is essential for the endocytosis of TLR4 and the consequent Toll-like receptor adaptor molecule-mediated interferon expression.<sup>3</sup> Intestinal TLR4 signaling can mediate inflammatory signals but can also promote tolerance to gut commensals and regulate the proliferation and differentiation of intestinal epithelial cells.<sup>4-7</sup> Dysfunctional TLR4 signaling may increase susceptibility to pathological intestinal inflammation.<sup>8-11</sup>

## RESULTS AND DISCUSSION

We identified biallelic truncating variants of *TLR4* in 2 siblings from a family of Qatari ancestry (a 22-year-old woman marked as IV.4, and a 14-year-old boy marked as IV.7) (Fig 1, A). The boy presented at age 11 years with complex perianal Crohn disease and wound healing problems (Fig 1, B; Table I). His sister (IV.4) showed no signs of susceptibility to infections or inflammation. Parents were healthy. A brother (IV.5) subsequently developed Crohn disease. Five further siblings in this family did not present with inflammatory or autoimmune disorders, or signs of immunodeficiency.

A homozygous TLR4 c.C562T variant predicted to result in early termination of the TLR4 protein (p.Q188X; CADD score of 35) was identified in IV.7 by whole-genome sequencing and in IV.4 by Sanger sequencing (see Fig E1, A and B, in this article's Online Repository at [www.jacionline.org](http://www.jacionline.org)). In a Qatari population data set,<sup>12</sup> the c.C562T TLR4 mean allele frequency (MAF) is low (MAF, 0.000899). In the Genome Aggregation Database (GnomAD) data set, the variant is even rarer (overall MAF, 0.000008; no homozygous individuals). Because the biallelic TLR4 deficiency in this family showed incomplete

penetrance and no segregation with the inflammatory phenotype, we considered the presence of additional causative variants shared between the affected brothers. Although 5 variants were heterozygous in the parents and homozygous in both the patient and his brother, their frequencies in the Qatari population data sets<sup>12,13</sup> are relatively high and none of them had corresponding plausible phenotypes in mouse knockout models (see Table E1 in this article's Online Repository at [www.jacionline.org](http://www.jacionline.org)).

To identify other individuals with TLR4 deficiency, we expanded our investigation to additional data sets. Investigation of approximately 120,000 alleles in the GnomAD browser revealed the presence of a third individual carrying a homozygous stop codon variant (c.C2382G; p.Y794X). The allele frequency of the p.Y794X variant is enriched in individuals of South Asian descent (MAF, 0.003). Interestingly, another loss-of-function (LOF) variant (p.N176FfsX27) has a similar MAF in the South Asian population (although no homozygotes are reported), suggesting that there may be positive selection of certain TLR4 variants in this population.

In total we identified 3 individuals with essential LOF, 2 carrying the variant p.Q188X and 1 p.Y794X. Both variants are encoded by exon 3, but the functional consequences of the 2 variants may differ (Fig 1, C). The wild-type (WT) TLR4 protein forms a membrane dimer that exposes a large extracellular leucine-rich domain,<sup>14</sup> whereas the p.Q188X variant truncates this extracellular domain with a small N-terminal fragment potentially remaining (Fig 2, A). This variant lacks the scaffold required to bind to myeloid differentiation factor 2 (MD2) and the ligands LPS or S100 proteins (Fig 2, B). In contrast, these interactions are potentially intact in the p.Y794X variant, which affects the intracellular C-terminal helix of TLR4 (Fig 2, C).

To study the variants functionally, we transfected HEK-Blue MD2-CD14 cells that lack endogenous TLR4 expression with plasmids encoding either the wild-type TLR4 or 1 of the TLR4 variants, p.Q188X or p.Y794X. We observed TLR4 surface staining on cells transfected with WT TLR4 but not on cells transfected with neither the p.Q188X nor the p.Y794X TLR4 variant (Fig 2, D).

Next, we examined I $\kappa$ B $\alpha$  levels (which inversely correlate with NF- $\kappa$ B activity) and assessed NF- $\kappa$ B activation using a reporter assay. On LPS stimulation, HEK293 cells transfected with WT TLR4 showed a significant reduction in I $\kappa$ B $\alpha$  levels, whereas I $\kappa$ B $\alpha$  levels were not altered in cells transfected with TLR4 p.Q188X or p.Y794X (Fig 2, E). For all the investigations in transfected cells, we made sure that the variants were expressed at a similar mRNA level as indicated by quantitative PCR (Fig 2, F).

We then wanted to compare the functional impact of essential LOF variants (identified in the Qatari family or in GnomAD) with 3 common polymorphisms in TLR4. Multiple studies have reported associations between TLR4 polymorphisms and inflammatory bowel disease (IBD). The 2 most widely studied TLR4 polymorphisms, p.D299G and p.T399I, affect the extracellular region of the TLR4 protein, impairing the binding with LPS and coreceptors.<sup>15,16</sup> In contrast to absent signaling caused by variants p.Q188X, p.Y794X, and the frameshift variant p.N176FfsX27 (second most abundant LOF TLR4 variant in GnomAD), the 3 polymorphisms p.T399I, p.D299G, and p.Y46C showed a slightly decreased level of NF- $\kappa$ B activation in the NF- $\kappa$ B reporter assay after LPS stimulation (Fig 2, G), suggesting a hypomorphic effect

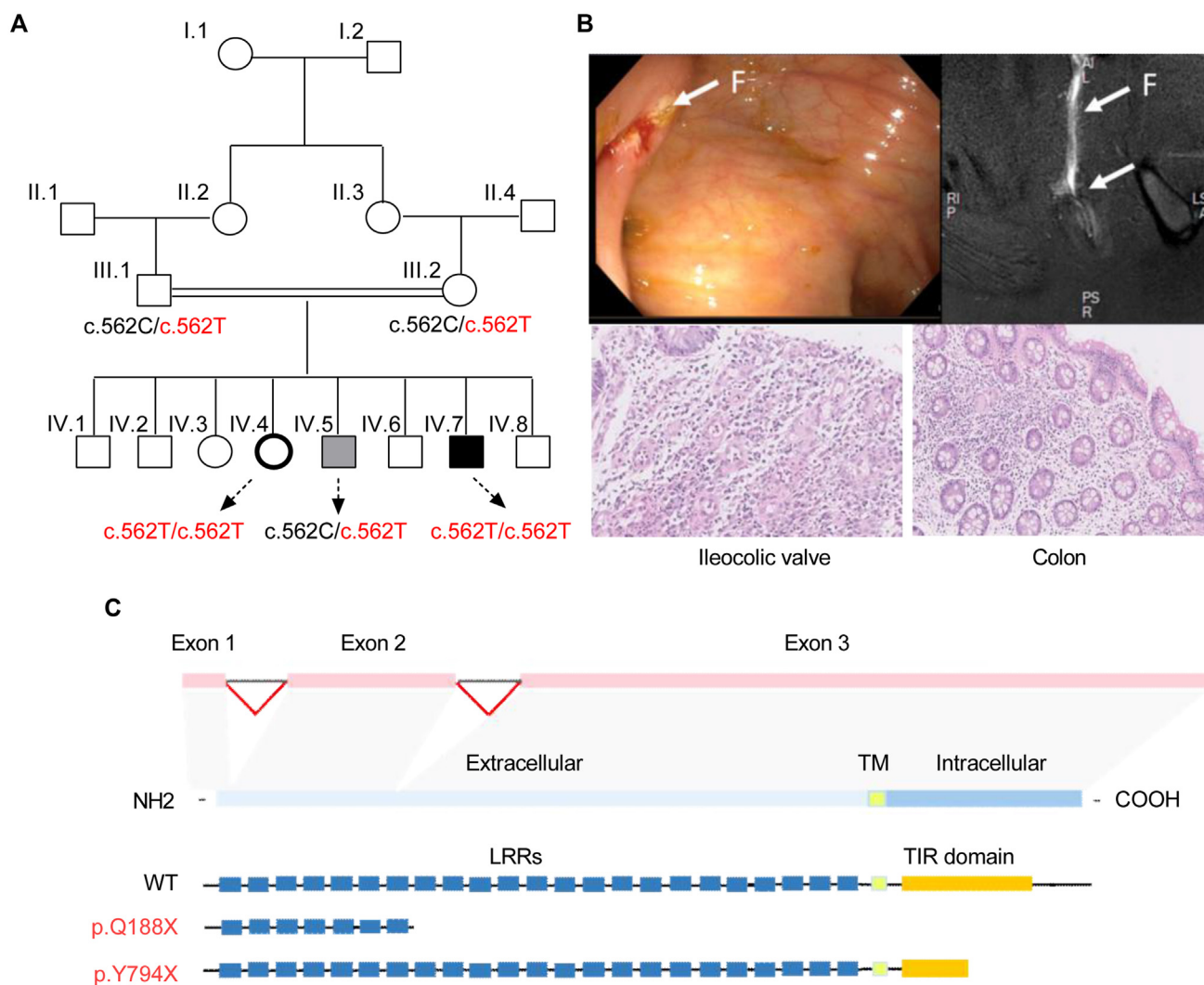


**FIG 1.** Biallelic essential TLR4 LOF variants in humans. **A**, Family tree of a consanguineous family with 2 children homozygous for c.562C>T (IV.4 and IV.7), whereas both parents and 1 son (IV.5) are heterozygous for the TLR4 variant c.562C>T. **B**, Gastrointestinal pathology of Crohn disease in an individual (IV.7) with homozygous TLR4 variant c.562C>T. Endoscopy and magnetic resonance imaging identify a fistula (white arrow - F). Hematoxylin and eosin-stained biopsies show signs of ileitis and colitis. **C**, Schematic representation of the *TLR4* gene with the 3 exons. The extracellular LRR domains, the transmembrane domain, and the intracellular TIR domain are highlighted in the TLR4 protein and the predicted consequences of the variants p.Q188X (encoded by c.562C>T) and the variant p.Y794X (encoded by c.2382C>G) are shown. *LRR*, Leucine-rich repeat; *TIR*, Toll-IL-1 receptor.

of the polymorphisms (see [Table E2](#) in this article's Online Repository at [www.jacionline.org](http://www.jacionline.org)).

We next investigated TLR4 signaling in primary cells of the family with homozygous TLR4 variants. PBMCs from the 2 siblings homozygous for p.Q188X were stained for TLR4, TLR2, and CD14. TLR4 surface protein expression in CD14<sup>+</sup> monocytes homozygous for p.Q188X was completely absent, whereas monocytes from the heterozygous parents and the brother IV.5 showed reduced levels of TLR4 expression compared with controls ([Fig 3, A](#)). In contrast to TLR4, the levels of TLR2 and CD14 ([Fig 3, B and C](#)) were similar to those in controls.

We then investigated the LPS response in monocytes. Monocytes of the 2 individuals homozygous for the TLR4 p.Q188X variant were unresponsive to LPS stimulation in the intracellular

tumor necrosis factor assay compared with controls or the heterozygous parents and brother (IV.5) ([Fig 3, D](#)). TLR2 responsiveness was not compromised by the loss of TLR4 ([Fig 3, E](#)). Neutrophils of the homozygous patient IV.7 had impaired CD62L shedding after LPS stimulation ([Fig 3, F and G](#)). This confirms a profound defect of TLR4-dependent LPS signaling in individuals with biallelic TLR4 p.Q188X variants.

Next, we investigated the LPS-induced cytokine secretion of isolated monocytes or PBMCs. In controls, stimulation of monocytes or PBMCs with LPS resulted in an increase in multiple cytokines (such as IL-6, IL-8, tumor necrosis factor, and IL1 $\alpha$ ), but not in the individuals with homozygous TLR4 p.Q188X variant ([Fig 4, A and B](#)). Interestingly, unstimulated monocytes and PBMCs from the patient IV.7 with homozygous

**TABLE I.** Phenotype and immune parameters of the index patient IV.7\*

**Phenotype:** The boy presented at age 11 years with recurrent fevers, vomiting, and persistent perianal pain from recurrent perianal abscesses. He was diagnosed with Crohn disease associated with complex perianal fistulizing disease (grade IV intrasphincteric fistula and branching fistula). Endoscopy identified ulcers at the ileocecal valve, cecum, and sigmoid colon. MRE and ultrasound showed wall thickening of the terminal ileum. Histologically, a giant cell local granuloma and a few patches of mild inflammation were identified in the terminal ileum (Fig 1, B). The patient underwent surgical drainage of the abscesses. Postoperatively he had poor wound healing with a persistent defect in his perianal area. Bacterial swab cultures from the wound showed mixed growth including enterobacteriales with extended spectrum beta-lactamases (*Escherichia coli* and gram-negative bacilli). Antibiotic treatment showed a good clinical response, and his fever resolved; while treatment with infliximab induced amelioration of a large defect in the skin in the perianal area and improvement of his inflammatory markers. Clinical immune profiling showed no abnormalities in neutrophil and lymphocyte counts or lymphocyte subsets but revealed elevated levels of IgA.

Complete blood cell count† ( $\times 10^9/L$ )		
Cell type	Value	Reference range
Neutrophil	3.8	0.8-7.2
Monocyte	0.6	0.1-1.1
Lymphocyte	2	1.3-8.0
Total immunoglobulin (g/L)		
Test	Value	Reference range
IgG	7.91	6.85-16.2
IgA	4.12 (H)	0.46-2.18
IgM	1.07	0.27-1.51
Lymphocyte subsets‡		
Markers	Value	Reference range
CD3	1506	800.00-3500.00
CD3 <sup>+</sup> /CD4 <sup>+</sup>	768	400.00-2100.00
CD3 <sup>+</sup> /CD8 <sup>+</sup>	663	200.00-1200.00
CD19	311	200.00-600.00
CD3 <sup>-</sup> /CD16/CD56 <sup>+</sup>	157	70.00-1200.00

H, Value is higher than the reference range.

MRE, Magnetic resonance enterography.

\*All tests were performed at age 11 y.

†Mean of absolute values of 8 tests over 6 mo.

‡Absolute values.

TLR4 p.Q188X variant showed high levels of PDGF-BB (a cytokine produced from activated macrophages) compared with cells from healthy controls and parents (Fig 4, C), suggesting a high baseline activation, but an absence of responsiveness to LPS.

Because defects in pathogen recognition can affect antimicrobial activity, we evaluated the capacity to clear bacteria in TLR4-deficient monocytes. Monocytes from the homozygous TLR4 p.Q188X variant male patient (IV.7), the heterozygous parents, and controls were infected with *Salmonella typhimurium*, at a multiplicity of infection (MOI) of 10. No differences were observed between the patient, parents, and controls, which suggests that the *TLR4* genotype does not impact the bacterial clearance capacity of monocytes (Fig 4, D).

Our data suggest that the loss of the pathogen recognition molecule TLR4 might be associated with pathological intestinal inflammation, but this can be compensated for by immunologic fail-safe mechanisms. The effects of TLR4 defects are therefore context-specific. TLR4-deficient mice do not develop spontaneous colitis but show increased epithelial barrier disruption after dextran sodium sulfate administration,<sup>17</sup> leading to enhanced bacterial translocation and increased bleeding compared with control mice. It is possible that the complete LOF variants in TLR4 described in this article might similarly contribute to inflammation and impaired tissue repair in the male patient (IV.7), who

has a fistulizing phenotype with recurrent perianal abscesses and poor wound healing. However, the incomplete penetrance and segregation of the variants prohibit a conclusive association, as demonstrated by the sister (IV.4), who had no immunologic phenotype, and the presence of TLR4 deficiency in a male older than 50 years in GnomAD.

Biallelic LOF variants in the coreceptor MD2 similarly predispose to Crohn disease with incomplete penetrance.<sup>18</sup> In contrast, defects in IRAK4 and MYD88 downstream of TLR signaling cause severe bacterial infections and immunodeficiency.<sup>19,20</sup> The greater severity and disease penetrance in MYD88 and IRAK4 deficiency can be attributed to their crucial role in mediating the signaling of multiple different TLRs/receptors. The allele frequency of 2 TLR4 essential LOF variants in Asian populations (p.Y794X and p.N176FfsX27, combined MAF ~0.5%) suggests that TLR4 LOF is evolutionarily less selected against compared with IRAK4 and MD88. This may indicate that TLR4 deficiency has a heterozygote advantage in some settings. It suggests that the host protective functions of TLR4 may be compensated, at least partially, by other mechanisms such as IRAK4 and MD88-dependent TLR2 signaling. Furthermore, it is notable that patients with IRAK4 and MYD88 deficiency do not typically develop IBD-like intestinal inflammation, indicating further differences in the immune phenotype between TLR4/MD2-restricted immunopathology

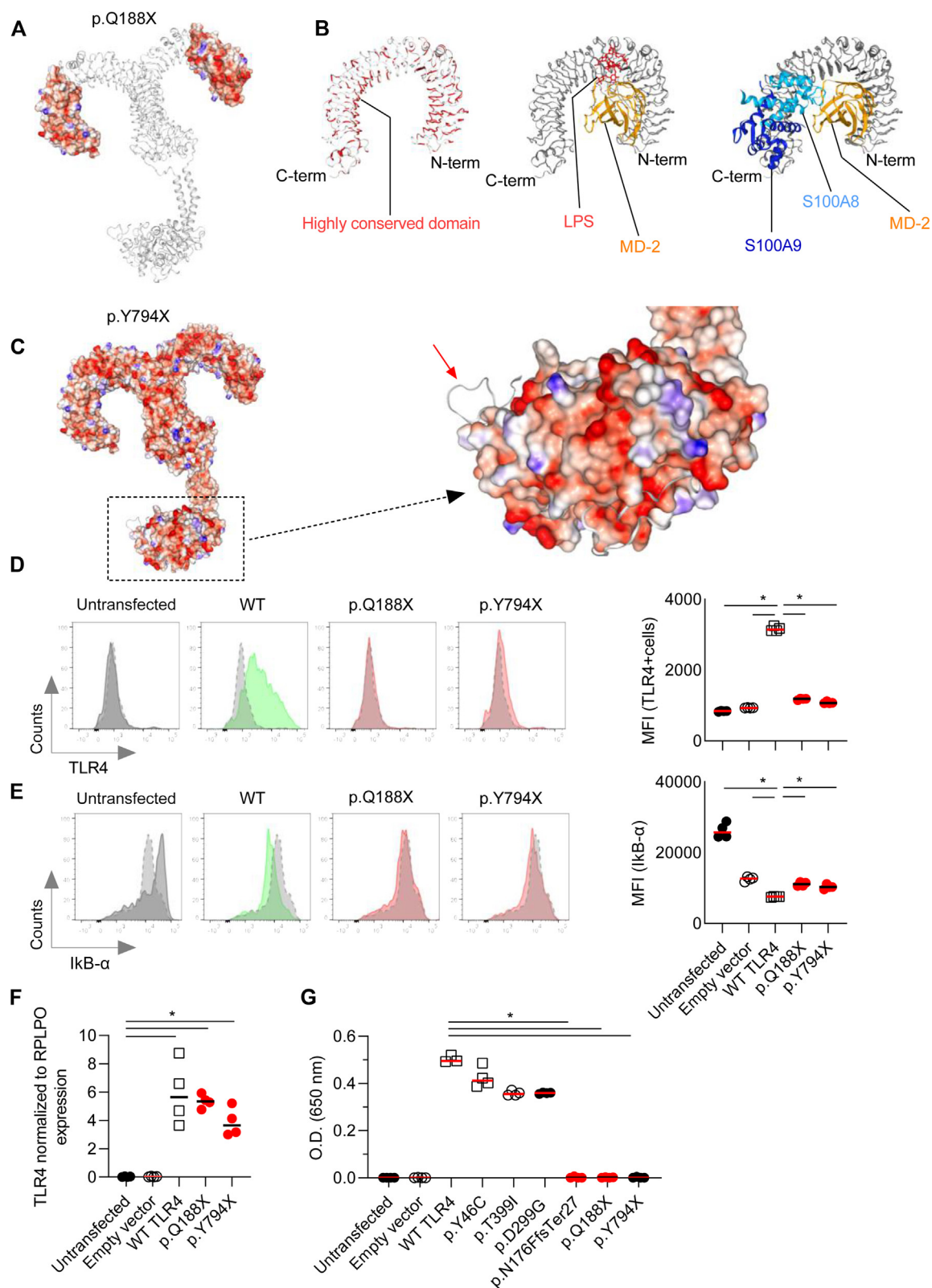


**FIG 2.** Structural consequences of the p.Q188X and p.Y794X variants and their impact on TLR4 surface expression and LPS responsiveness in HEK293-cell *in vitro* model. **A**, Predicted structure of TLR4 with p.Q188X variant and deleted (gray structure view) region. **B**, Evolutionary conservation (red), interactions with MD2 and LPS; and interactions with MD2, S100A8/S100A9. **C**, Predicted structure of p.Y794X variant and deleted region (gray structure indicated by the arrow). **D-G**, HEK-blue cell transfection experiments. Dashed overlay plots represent the empty vector condition: **D**, TLR4 surface expression (n = 4 replicates). **E**, IκB-α levels on LPS (n = 4 replicates). **F**, TLR4 mRNA expression in HEK-blue cells after transfection. **G**, Colorimetric NF-κB reporter assay. *MFI*, Median fluorescence intensity. Statistical significance was determined using Mann-Whitney *U* test. \**P* < .05.

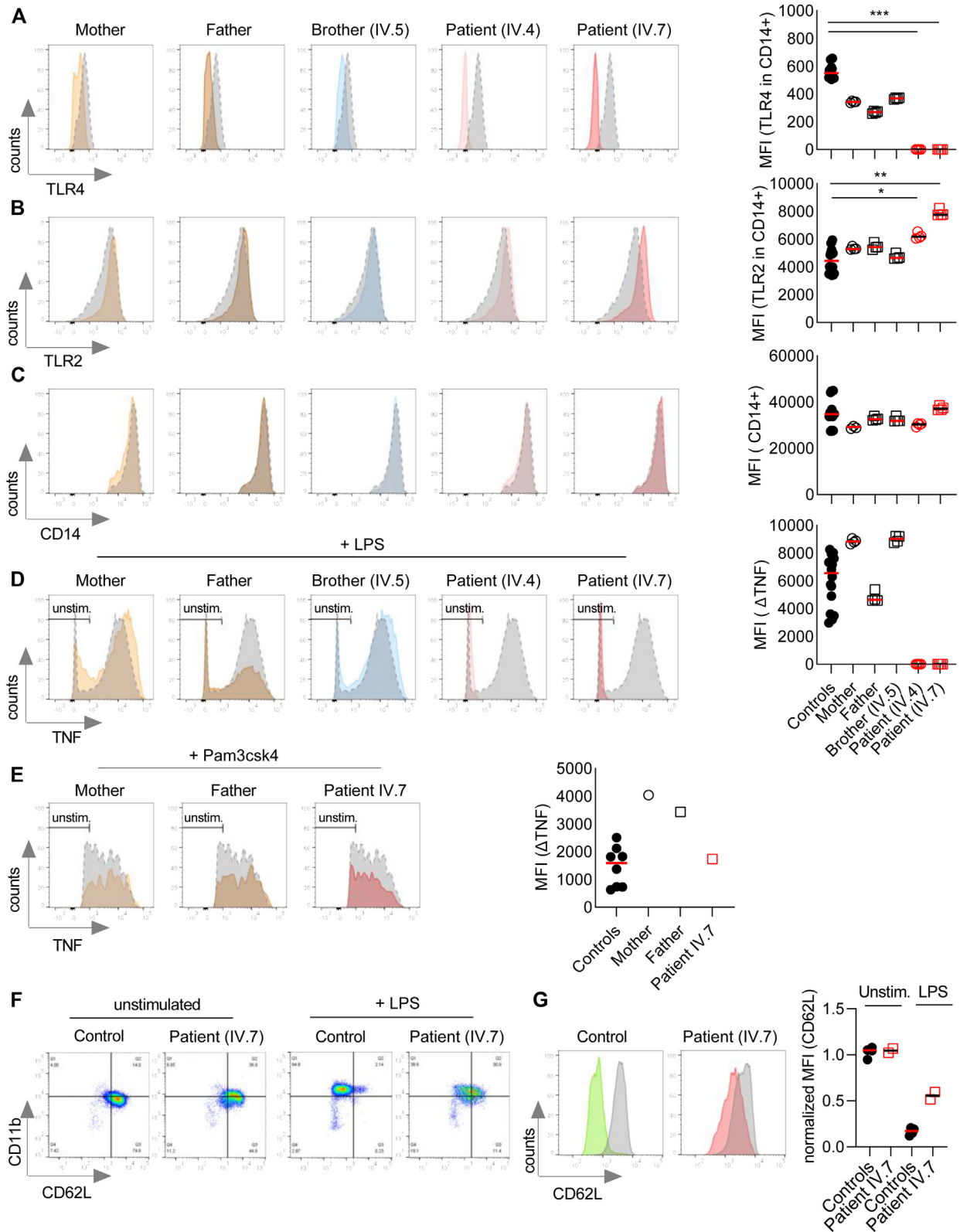


**FIG 3.** Homozygous TLR4 p.Q188X abrogates TLR4 surface expression and responsiveness to LPS in primary human monocytes. **A-C**, Surface expression of TLR4 (Fig 3, **A**), TLR2 (Fig 3, **B**), and CD14 (Fig 3, **C**) on CD14<sup>+</sup> monocytes of the 2 homozygous individuals (IV.4 and IV.7) and 3 heterozygous family members (mother, father, brother IV.5). **D**, Intracellular TNF in CD14<sup>+</sup> monocytes stimulated with LPS. **E**, Intracellular TNF production on Pam3csk4 stimulation in monocytes. In all plots, the healthy control was overlaid as a comparison (dashed line). **F**, CD62L and CD11b surface expression in granulocytes of patient IV.7 compared with a representative control, at baseline and after LPS stimulation. **G**, CD62L surface expression after LPS stimulation. Gray plot represents the unstimulated condition. *MFI*, Median fluorescence intensity; *TNF*, tumor necrosis factor; *Unstim*, unstimulated. Statistical significance was determined using Kruskal-Wallis test. \**P* < .05.

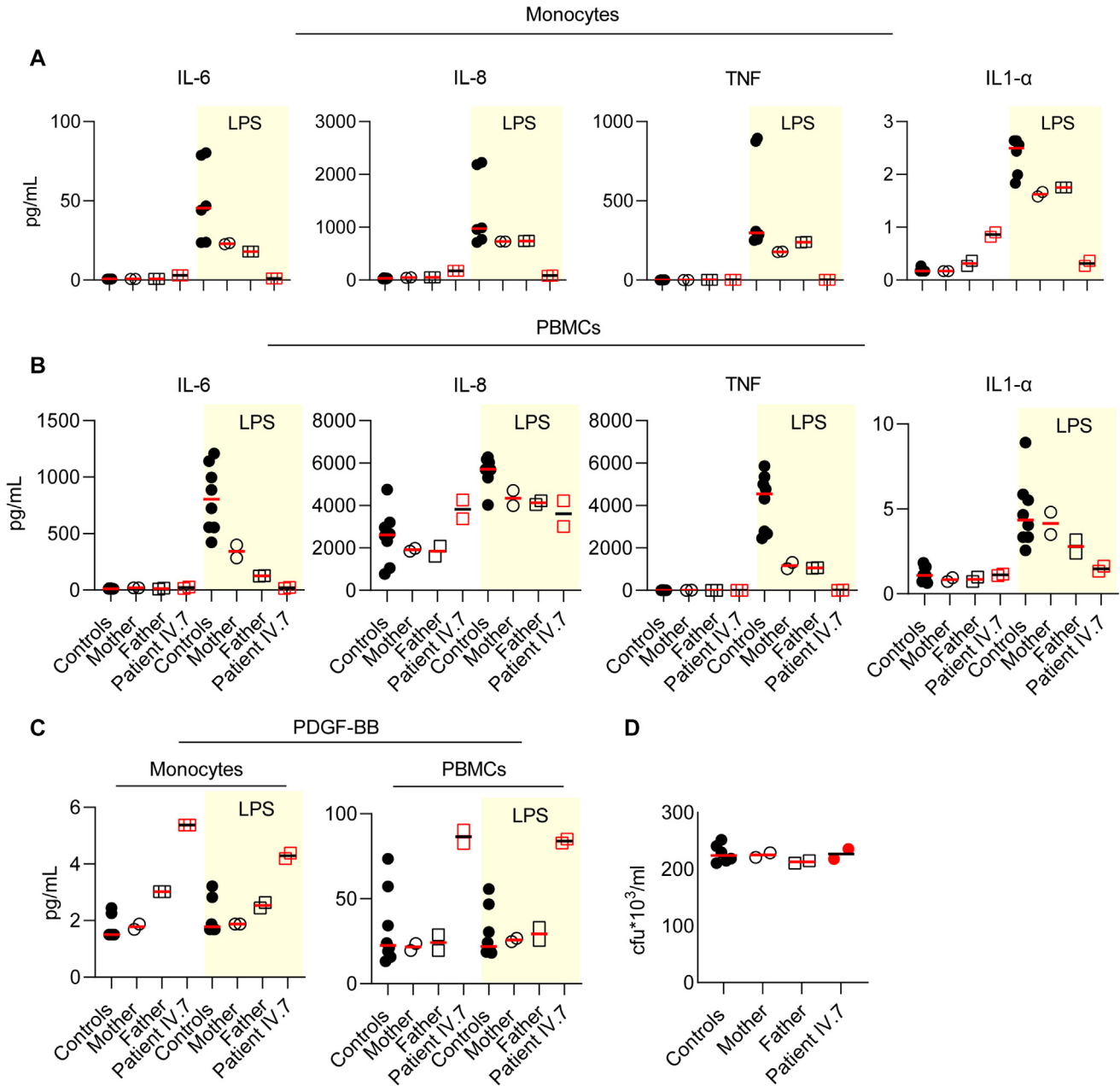


**FIG 4.** TLR4 deficiency abrogates cytokine responses but maintains antimicrobial activity. **A**, Cytokines from monocytes of the homozygous individual IV.7, heterozygous individuals (mother and father), and healthy controls left unstimulated or stimulated with LPS (yellow highlight). **B**, Cytokines in unstimulated or LPS-stimulated PBMCs. **C**, PDGF-BB production from unstimulated or stimulated monocytes or PBMCs. **D**, *Salmonella* colonies resulting from viable intracellular bacteria as quantified by the gentamicin protection assay.

and defects in IRAK4 and MYD88. Altogether, the Crohn disease phenotype in patients with TLR4 and MD2 deficiency,<sup>18</sup> IBD-associated TLR4 polymorphisms, and model systems<sup>17</sup> supports the role of context-specific TLR4 signaling as a susceptibility factor for IBD.

We thank the patients, family, and sample donors for participating in this study. We also thank the Sidra Medicine Genomics Core and the Sidra

Bioinformatics Team, notably Hakeem Almazrazi and Fazlur Rehman Vempalli, for technical support. We acknowledge Melanie Dunstan who contributed to collection of samples in Oxford. We thank Ruslan Medzhitov for sharing the pCDNA3.1-hTLR4 (Addgene plasmid #13086). We acknowledge the contribution of the Oxford GI biobank (11/YH/0020, 16/YH/0247) and thank all investigators of the Oxford GI biobank. This study includes data generated by the Qatar Genome Programme (QGP) and Qatar Biobank (QBB), which are funded by Qatar Foundation for Education, Science and Community, and we thank all investigators of the QGP and QBB.

We thank all investigators of the COLORS in IBD study group in particular the COLORS in IBD-Qatar study group investigators at Hamad Medical Corporation, and Sidra Medicine, Doha, Qatar.

**Clinical implications: TLR4 deficiency has a variable phenotype and can be present in asymptomatic individuals.**

## REFERENCES

1. Medzhitov R, Preston-Hurlburt P, Janeway CA Jr. A human homologue of the *Drosophila* Toll protein signals activation of adaptive immunity. *Nature* 1997; 388:394-7.
2. Vogl T, Tenbrock K, Ludwig S, Leukert N, Ehrhardt C, van Zoelen MA, et al. Mrp8 and Mrp14 are endogenous activators of Toll-like receptor 4, promoting lethal, endotoxin-induced shock. *Nat Med* 2007;13:1042-9.
3. Tsukamoto H, Takeuchi S, Kubota K, Kobayashi Y, Kozakai S, Ukai I, et al. Lipopolysaccharide (LPS)-binding protein stimulates CD14-dependent Toll-like receptor 4 internalization and LPS-induced TBK1-IKK-IRF3 axis activation. *J Biol Chem* 2018;293:10186-201.
4. Naito T, Mulet C, De Castro C, Molinaro A, Saffarian A, Nigro G, et al. Lipopolysaccharide from crypt-specific core microbiota modulates the colonic epithelial proliferation-to-differentiation balance. *mBio* 2017;8:e01680-17.
5. Burgueno JF, Abreu MT. Epithelial Toll-like receptors and their role in gut homeostasis and disease. *Nat Rev Gastroenterol Hepatol* 2020;17:263-78.
6. Rakoff-Nahoum S, Paglino J, Eslami-Varzaneh F, Edberg S, Medzhitov R. Recognition of commensal microflora by toll-like receptors is required for intestinal homeostasis. *Cell* 2004;118:229-41.
7. Abreu MT, Arnold ET, Thomas LS, Gonsky R, Zhou Y, Hu B, et al. TLR4 and MD-2 expression is regulated by immune-mediated signals in human intestinal epithelial cells. *J Biol Chem* 2002;277:20431-7.
8. Dheer R, Santaolalla R, Davies JM, Lang JK, Phillips MC, Pastorini C, et al. Intestinal epithelial Toll-like receptor 4 signaling affects epithelial function and colonic microbiota and promotes a risk for transmissible colitis. *Infect Immun* 2016;84:798-810.
9. Lu Y, Li X, Liu S, Zhang Y, Zhang D. Toll-like receptors and inflammatory bowel disease. *Front Immunol* 2018;9:72.
10. Matharu KS, Mizoguchi E, Cotoner CA, Nguyen DD, Mingle B, Iweala OI, et al. Toll-like receptor 4-mediated regulation of spontaneous *Helicobacter*-dependent colitis in IL-10-deficient mice. *Gastroenterology* 2009;137:1380-90.e1-3.
11. Shi YJ, Hu SJ, Zhao QQ, Liu XS, Liu C, Wang H. Toll-like receptor 4 (TLR4) deficiency aggravates dextran sulfate sodium (DSS)-induced intestinal injury by down-regulating IL6, CCL2 and CSF3. *Ann Transl Med* 2019;7:713.
12. Fakhro KA, Staudt MR, Ramstetter MD, Robay A, Malek JA, Badii R, et al. The Qatar genome: a population-specific tool for precision medicine in the Middle East. *Hum Genome Var* 2016;3:16016.
13. Al Thani A, Fthenou E, Paparrodopoulos S, Al Marri A, Shi Z, Qafoud F, et al. Qatar Biobank Cohort Study: study design and first results. *Am J Epidemiol* 2019;188:1420-33.
14. Patra MC, Kwon HK, Batoool M, Choi S. Computational insight into the structural organization of full-length Toll-like receptor 4 dimer in a model phospholipid bilayer. *Front Immunol* 2018;9:489.
15. Shen X, Shi R, Zhang H, Li K, Zhao Y, Zhang R. The Toll-like receptor 4 D299G and T399I polymorphisms are associated with Crohn's disease and ulcerative colitis: a meta-analysis. *Digestion* 2010;81:69-77.
16. Senhaji N, Diakite B, Serbati N, Zaid Y, Badre W, Nadifi S. Toll-like receptor 4 Asp299Gly and Thr399Ile polymorphisms: new data and a meta-analysis. *BMC Gastroenterol* 2014;14:206.
17. Fukata M, Michelsen KS, Eri R, Thomas LS, Hu B, Lukasek K, et al. Toll-like receptor-4 is required for intestinal response to epithelial injury and limiting bacterial translocation in a murine model of acute colitis. *Am J Physiol Gastrointest Liver Physiol* 2005;288:G1055-65.
18. Li Y, Yu Z, Schenk M, Lagovsky I, Illig D, Walz C, et al. Human MD2 deficiency—an inborn error of immunity with pleiotropic features. *J Allergy Clin Immunol* [E-pub ahead of print]. <https://doi.org/10.1016/j.jaci.2022.09.033>.
19. Picard C, von Bernuth H, Ghandil P, Chrabieh M, Levy O, Arkwright PD, et al. Clinical features and outcome of patients with IRAK-4 and MyD88 deficiency. *Medicine (Baltimore)* 2010;89:403-25.
20. Gobin K, Hintermeyer M, Boisson B, Chrabieh M, Ghandil P, Puel A, et al. IRAK4 deficiency in a patient with recurrent Pneumococcal infections: case report and review of the literature. *Front Pediatr* 2017;5:83.



## METHODS

### Patient cohort and ethics

This study was approved by the Oxford GI biobank (ethics no. 09/H1204/30) and Sidra Medicine Institutional Review Board (IRB protocol 1601002512). Written informed consent was obtained from parents and healthy controls, with local ethics approval (REC 11/LO/0330).

### Genome sequencing and variant validation

DNA from patients and parents were whole-genome-sequenced to an average of 30-fold coverage, using an Illumina HiSeq X platform. Burrows-Wheeler Aligner was used to align reads to the hg19 human reference, and GATK HaplotypeCaller was used for variant and indel calling. GATK Variant Quality Score Recalibration was used for variant quality filtering. Variant Call Format (VCF) files were annotated with SnpEff/SnpSift. Variants were filtered and prioritized on the basis of quality scores, recessive or *de novo* mode of inheritance, allele frequency lower than 0.005 in the 1000 Genomes Project (1000GP) or GnomAD, predicted deleteriousness (SIFT, PolyPhen, MutationTaster), and functional relevance to the patient phenotype. Variants that were homozygous in GnomAD or 1000GP were not considered (Fig E1, A).

Based on a model of possible recessive inheritance, homozygous variants in both index patient IV.7 and brother IV.5 were further assessed for allele frequency and the presence of homozygotes in the Qatari population data sets (Table E1). Homozygotes for these variants were present, suggesting that they may not be causative of a highly penetrant monogenic disorder. Literature review of the 5 genes found that the ones with reported mouse knockout phenotypes were not relevant to the disease of our patients.

The TLR4 nonsense variant was confirmed in the patient by Sanger sequencing using purified PCR products amplified by the following primers: 5'-CTTAATGTGGCTCACAAATCTTATCC-3' and 5'-TTCATAGGGTT CAGGACAGG-3' (Fig E1, B). For the p.Y794X (c.C2382G) variant identified from the GnomAD data set, genome screening was performed by GATK HaplotypeCaller-bamOutput (Fig E1, C).

### TLR4 isoform expression and variant analysis

The 4 TLR4 isoforms, resulting from the alternative splicing, have been investigated for their expression in different tissue by using the GTEx portal (<https://gtexportal.org/home/>).

To investigate the allele frequencies of TLR4 variants, the following online data sources have been accessed: 1000 Genomes (<http://www.1000genomes.org>), GenBank (<http://www.ncbi.nlm.nih.gov>), GnomAD (<http://gnomad.broadinstitute.org>), ExAC browser (<http://exac.broadinstitute.org>), 100K Genome project (<https://100kgenomes.org>), Inflammatory Bowel Disease Exomes Browser (<https://ibd.broadinstitute.org/0>), and Decipher GRCh37-DDD study (<https://decipher.sanger.ac.uk>).

### Variant modeling

Construction of a 3-dimensional model of the full-length TLR4 molecule in association with MD2 in the cell membrane has previously been described.<sup>E7</sup> This model was visualized using the web-based application MichelaN-GLO<sup>E8,E9</sup> and used to map the p.Gln188Ter and p.Tyr794Ter variants.

The extracellular TLR4 domain in complex with MD-2 and LPS was obtained from the protein databank<sup>E10,E11</sup> cryo-electron microscopy structural entry 3FXI.<sup>E12</sup> The degree of conservation of amino acid residues within the extracellular domain was assessed using the ConSurf web server (<http://consurf.tau.ac.il>).<sup>E13,E14</sup> Normalized conservation scores for each amino acid were calculated. Residues with a conservation score of less than -0.41 were highlighted as conserved and mapped to the TLR4 extracellular domain using MichelaN-GLO. The TLR4 extracellular domain in association with S100A8/S100A9 proteins was derived from docking experiments previously described.<sup>E15</sup>

### Plasmid transfection and NF-κB reporter assay

HEK-Blue MD2-CD14 (InvivoGen, San Diego, Calif) stably express the genes for the 2 coreceptors of TLR4, MD-2 and CD14, and an NF-κB/AP1-

inducible secreted embryonic alkaline phosphatase reporter gene. Cells were cultured in presence of Dulbecco modified Eagle medium with 10% FBS, 1% penicillin/streptomycin, and selection antibiotics (Zeocin 100 μg/mL and Hygromycin B gold 200 ng/mL; InvivoGen). Cells were plated at a concentration of  $2 \times 10^6$  in a 10-cm plate and transfected after 48 hours with pCDNA3.1-hTLR4 WT (#13086; Addgene) or with pCDNA3.1-hTLR4 (carrying or the c.C562T mutation or the c.C2382G obtained from GenScript). Cells transfected with an empty plasmid (pCDNA3.1) and untransfected cells were used as control. Twenty-four hours posttransfection, cells were detached by pipetting and plated at a concentration of  $4 \times 10^4$  cells per well in a 96-well plate in the presence of the Detection Media (InvivoGen) containing secreted embryonic alkaline phosphatase color substrate. Cells were stimulated with LPS 100 ng/mL overnight. Unstimulated cells were used as control. The absorbance of the supernatant was read at the spectrophotometer at the wavelength of 655 nm.

For comparison, we selected 4 TLR4 variants: 3 polymorphisms and 1 additional essential LOF variant (Table E2). We then performed the NF-κB colorimetric assay as described above with HEK-Blue MD2-CD14 cells transfected with pCDNA3.1-hTLR4 carrying the c.A896G mutation (p.Asp299Gly) or the c.C1196T mutation (p.Thr399Ile) or the c.A137G mutation (p.Tyr46Cys) or the c.AA526-527TT mutation (p.Asn176Phef-sTer27). These plasmids were provided by GenScript.

### Quantitative TLR4 expression

Total RNA was extracted from monocytes and from transfected Hek-Blue MD2-CD14 cells. mRNA was then retrotranscribed to cDNA using High-Capacity cDNA Reverse Transcriptase (Applied Biosystems, Life Technologies, Waltham, Mass). The QPCR to investigate the levels of expression of TLR4 was carried out by using TaqMan Master Mix and TaqMan gene-specific probes (Life Technologies) and normalized to the house-keeping gene RPLPO (Hs00420895\_gH). The probe used for TLR4 (Hs00152939\_m1) recognizes both the WT and the 2 mutant sequences.

### Surface marker staining and ligand stimulation experiments

PBMCs were isolated by density gradient centrifugation (Lymphoprep; StemCell Technologies, Inc, Vancouver, British Columbia, Canada). Cells were then frozen in the presence of 90% FBS and 10% dimethyl sulfoxide and stored in liquid nitrogen.

Once defrosted, the cells were counted and plated in a 96-U-bottom-well plate at a concentration of  $5 \times 10^5$  cells per well in presence of RPMI1640 medium with glutamine (Sigma-Aldrich, St Louis, Mo) and 10% FBS. After resting overnight, some wells of PBMCs were stimulated for 3 hours, with LPS (200 ng/mL), or Pam3csk4 (2 μg/mL) in presence of Brefeldin A (1:1000), followed by surface marker staining with antibody to CD14 (clone MSE2, BioLegend, San Diego, Calif), CD19 (Clone HIB19, BioLegend), CD3 (Clone UCHT1, Biolegend), CD4 (Clone SK3, Biolegend), TLR2 (Clone FAB2616A, R&D Systems, Minneapolis, Minn), TLR4 (Clone TF901, BD Biosciences, Franklin Lakes, NJ), CD80 (Clone 2D10, Biolegend), and HLA-DR (Clone L243, eBioscience, San Diego, Calif). Investigation of the intracellular tumor necrosis factor was performed with the anti-tumor necrosis factor antibody (Clone Mab11, eBioscience). Cell viability was addressed by passive staining with Fixable Viability dye (Invitrogen, Waltham, Mass).

NF-κB activation was measured by IκB-α degradation. Cells were also stimulated with 200 ng/mL of LPS for 2 hours and stained with antibody anti-IκB-α (1:500 clone L35A5, Cell Signaling, Danvers, Mass) followed by a secondary antibody antimouse Bv650 (1:300, clone RMG1-1, BD). Levels of IκB-α were then assessed by cytofluorimetry.<sup>E16</sup>

For the CD62L shedding assay, buffy coat was isolated from fresh blood collected using Vacutainer ACD Tubes (Becton Dickinson, Franklin Lakes, NJ) by centrifugation at 400 RCF for 10 minutes. Isolated cells were resuspended in Advanced RPMI (Thermo Fisher Scientific, Waltham, Mass) supplemented with L-glutamine and 20% FBS in the same volume as the initial blood collection. Stimulation was performed in duplicates using 200 μL of

cell suspension per replicate. Cells were challenged with 200 ng/mL of LPS from *Escherichia coli* K-235 (Sigma, St Louis, Mo) for 30 minutes at 37°C and 5% CO<sub>2</sub>. Cells were then placed on ice for 1 hour to stop ongoing reactions and to stain with antibodies against CD62L (clone IM1231U, Beckman Coulter, Brea, Calif), CD3 (clone 555333, BD Pharmingen, San Diego, Calif), CD14 (clone 325614, Biolegend), and CD11b/Mac-1 (clone 550019, BD Pharmingen). Cells were washed twice by centrifugation using a cold swing-bucket centrifuge and ice-cold PBS followed by lysis using BD FACS lysing solution (Becton Dickinson) according to manufacturer recommendations. Cells were then fixed using 4% paraformaldehyde in PBS for 20 minutes at room temperature. Cells were then washed and analyzed by flow cytometry.

### Gentamicin protection assay

Gentamicin protection assay was performed, essentially as previously described.<sup>E17</sup> Monocytes from the patient, the parents, and healthy donor controls were plated in 96-well plate and left to rest overnight. The following day, cells were infected with *Salmonella typhimurium*, MOI 10, to address the ability of these cells to eliminate invading bacteria.

### Cytokine quantification

Monocytes and PBMCs of the patient, parents, and controls were stimulated for 3 hours with LPS 100 ng/mL or left unstimulated. Supernatants were collected and assayed, without any dilution, according to the standard procedure of the Magnetic Luminex Assay (R&D Systems). Samples were investigated for the levels of the following cytokines: IFN- $\gamma$ , MCP-1, IL-1 $\beta$ , IL-8, IL-12, IL-23, TNF, IP-10, IL-1 $\alpha$ , IL-6, IL-10, IL-18, and PDGF-BB. The samples were acquired by MAGPIX machine. The concentration of each cytokine in each sample was calculated directly from the MAGPIX machine software based on the concentration of the standards.

### Statistics

Graphs and statistical analysis were generated using Prism Version 8 (GraphPad, San Diego, Calif). All experiments were repeated as a minimum in triplicate unless otherwise specified. Differences of groups were investigated using nonparametric Mann-Whitney test. *P* less than .05 was considered significant.

### REFERENCES

- E1. Taylor GA, Rodriguiz RM, Greene RI, Daniell X, Henry SC, Crooks KR, et al. Behavioral characterization of P311 knockout mice. *Genes Brain Behav* 2008;7:786-95.
- E2. Liao Y, Tham DKL, Liang FX, Chang J, Wei Y, Sudhir PR, et al. Mitochondrial lipid droplet formation as a detoxification mechanism to sequester and degrade excessive urothelial membranes. *Mol Biol Cell* 2019;30:2969-84.
- E3. Kwon YT, Xia Z, An JY, Tasaki T, Davydov IV, Seo JW, et al. Female lethality and apoptosis of spermatocytes in mice lacking the UBR2 ubiquitin ligase of the N-end rule pathway. *Mol Cell Biol* 2003;23:8255-71.
- E4. <https://www.mousephenotype.org/data/genes/MGI:1923291>. Accessed August 2022.
- E5. <https://www.mousephenotype.org/data/genes/MGI:1914105>. Accessed August 2022.
- E6. Fakhro KA, Staudt MR, Ramstetter MD, Robay A, Malek JA, Badii R, et al. The Qatar genome: a population-specific tool for precision medicine in the Middle East. *Hum Genome Var* 2016;3:16016.
- E7. Patra MC, Kwon HK, Batool M, Choi S. Computational insight into the structural organization of full-length Toll-like receptor 4 dimer in a model phospholipid bilayer. *Front Immunol* 2018;9:489.
- E8. Ferla MP, Pagnamenta AT, Damerell D, Taylor JC, Marsden BD, MichelaNglo: sculpting protein views on web pages without coding. *Bioinformatics* 2020;36:3268-70.
- E9. Rose AS, Bradley AR, Valasatava Y, Duarte JM, Prlic A, Rose PW. NGL viewer: web-based molecular graphics for large complexes. *Bioinformatics* 2018;34:3755-8.
- E10. Berman HM, Bhat TN, Bourne PE, Feng Z, Gilliland G, Weissig H, et al. The Protein Data Bank and the challenge of structural genomics. *Nat Struct Biol* 2000;7:957-9.
- E11. Berman H, Henrick K, Nakamura H. Announcing the worldwide Protein Data Bank. *Nat Struct Biol* 2003;10:980.
- E12. Park BS, Song DH, Kim HM, Choi BS, Lee H, Lee JO. The structural basis of lipopolysaccharide recognition by the TLR4-MD-2 complex. *Nature* 2009;458:1191-5.
- E13. Landau M, Mayrose I, Rosenberg Y, Glaser F, Martz E, Pupko T, et al. ConSurf 2005: the projection of evolutionary conservation scores of residues on protein structures. *Nucleic Acids Res* 2005;33:W299-302.
- E14. Ashkenazy H, Abadi S, Martz E, Chay O, Mayrose I, Pupko T, et al. ConSurf 2016: an improved methodology to estimate and visualize evolutionary conservation in macromolecules. *Nucleic Acids Res* 2016;44:W344-50.
- E15. Vogl T, Stratis A, Wixler V, Voller T, Thurainayagam S, Jorch SK, et al. Autoinhibitory regulation of S100A8/S100A9 alarmin activity locally restricts sterile inflammation. *J Clin Invest* 2018;128:1852-66.
- E16. Oeckinghaus A, Wegener E, Welteke V, Ferch U, Çöl Arslan S, Ruland J, et al. Malt1 ubiquitination triggers NF- $\kappa$ B signaling upon T-cell activation. *EMBO J* 2007;26:4634-45.
- E17. Schwerdt T, Pandey S, Yang HT, Bagola K, Jameson E, Jung J, et al. Impaired antibacterial autophagy links granulomatous intestinal inflammation in Niemann-Pick disease type C1 and XIAP deficiency with NOD2 variants in Crohn's disease. *Gut* 2017;66:1060-73.

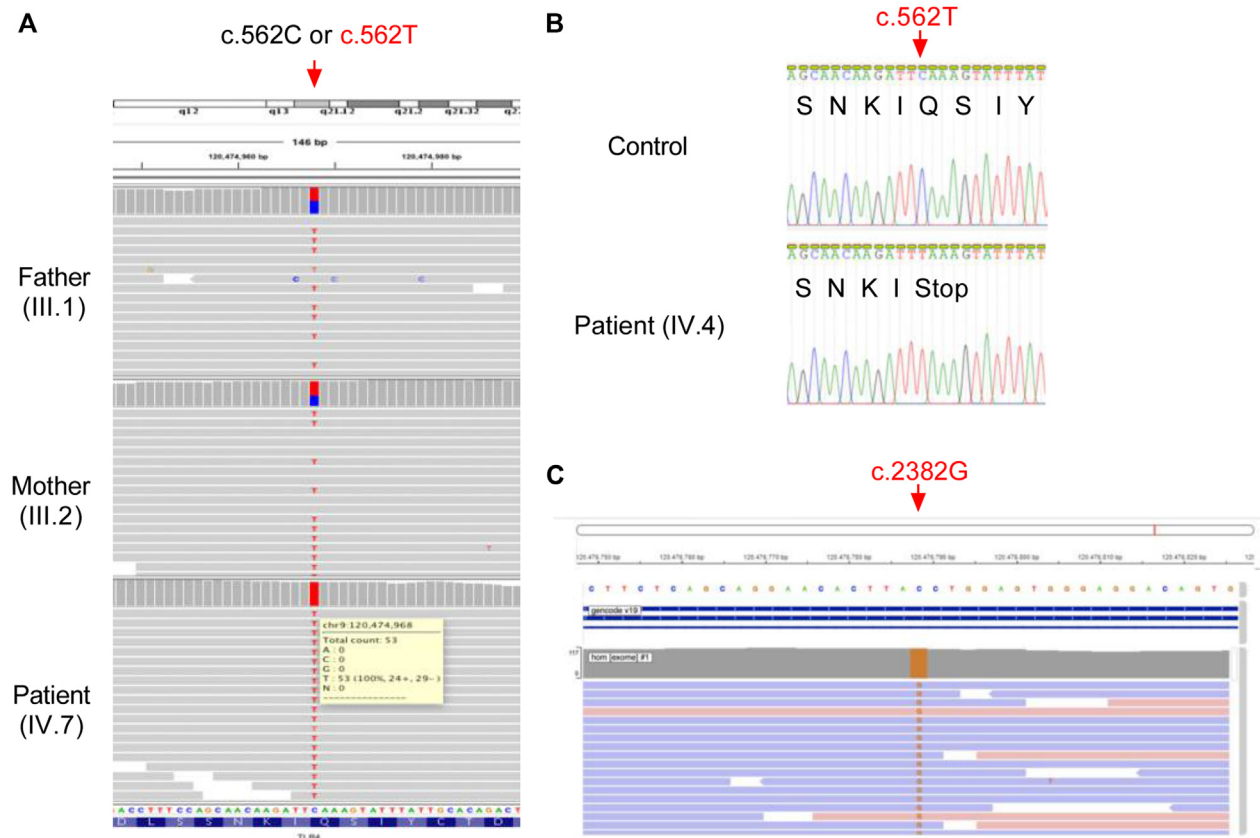


**FIG E1.** TLR4 variants screening. **A**, Whole-genome sequencing shows homozygosity for the variant c.562C>T in the TLR4 gene of IV.7; while the parents are heterozygous. **B**, Sanger sequencing analysis of c.562C>T from IV.4 in comparison to a healthy control. **C**, Whole-genome sequencing results from the GnomAD data set identify homozygosity of the LOF variant, c. 2382C>G.

**TABLE E1.** Rare homozygous variants shared in the index patient IV.7 and brother IV.5

Gene	Variant	GnomAD MAF	QTRG		QGP		KO phenotype (reference)
			MAF	No. of homo*	MAF	No. of homo*	
NREP	c.178T>A; p.Phe60Ile	0	0	0	0.001398	1	Behavior demonstrating impaired learning and memory processes and emotional responses <sup>E1</sup>
SNX31	c.831T>G; p.Cys277Trp	0.0001580	0.002248	1	0.001295	0	Disruption of multivesicular bodies in urothelial umbrella cells <sup>E2</sup>
UBR2	c.2768G>A; p.Arg923Lys	0	0.0008993	0	0.002488	2	Prenatal lethality depending on sex and strain background; degeneration of testes; impaired fertility <sup>E3</sup>
CCDC125	c.1018C>G; p.Gln340Glu	0.00007492	0.005845	0	0.008487	5	Tremors and long tibia <sup>E4</sup>
TCF25	c.1249C>T; p.Leu417Phe	0.00002743	0.021	2	0.01861	16	Thrombocytopenia, enlarged kidney, small testis, & increased freezing behavior <sup>E5</sup>

QGP, Qatar Genome Programme (<https://qatargenome.org.qa>); QTRG, a publicly available Qatari population genomic data set.<sup>E6</sup>

\*Homo, Homozygotes in the indicated population data set.

**TABLE E2.** Additional TLR4 variants with their characteristics

Variant	Predicted effect	GnomAD MAF	No. of homozygotes	Clinical significance
c.A137G p.Tyr46Cys	Missense	$2.41 \times 10^{-3}$	5	Unknown
c.C1196T p.Thr399Ile	Missense	$5.60 \times 10^{-2}$	584	Benign
c.A896G	Missense	$6.12 \times 10^{-2}$	658	Benign, protective
p.Asp299Gly				
c.AA526-527TT p.Asn176PhefsTer27	Frameshift	$3.35 \times 10^{-4}$	0	Unknown

Info from [https://gnomad.broadinstitute.org/gene/ENSG00000136869?dataset=gnomad\\_r2\\_1](https://gnomad.broadinstitute.org/gene/ENSG00000136869?dataset=gnomad_r2_1).